Dynamic Soil Structure Interaction with SBFEM

MSc. Bojan Radmanovic, Prof. Dr.-Ing. Casimir Katz, SOFiSTiK AG

Zusammenfassung:
Für die Behandlung der Boden-Bauwerks-Wechselwirkungen gibt es eine Vielzahl von Möglichkeiten. Diese kann man grob in zwei Verfahren unterteilen. Bei der direkten Methode wird der Boden ebenfalls mit Finiten Elementen definiert, das Problem entsteht bei der Formulierung der Randbedingung an den äußeren Rändern, wohingegen bei der Methode der Unterstrukturen versucht wird, das Verhalten des unendlichen Halbraums analytisch in den Griff zu bekommen. Die Methode der „Scaled Boundary Finite Elements" nimmt eine Zwischenstellung ein. Bis jetzt hatte die Methode einen gravierenden Nachteil: Die Lösung erfordert voll besetzte Matrizen und die Auswertung eines Faltungsintegrals und war damit außerordentlich rechenaufwändig. Mit den neuesten Entwicklungen steht nun aber ein einsetzbares Werkzeug zur Verfügung, dass die Behandlung dieser Probleme erlaubt.

1. Introduction

To illustrate the effects of dynamic soil-structure interaction (SSI) let us have a look at an example - the building to the left of the *Figure 1*. Various dynamic loading can act on a building. For example, seismic waves can propagate trough soil, causing it to oscillate. The oscillation of the soil is different when the building with the foundation is present from the free-field solution of the soil when the structure is not present. This is the first glimpse on the dynamic soil-structure interaction. When the seismic wave front reaches the foundation it causes the building to vibrate. Excited, building emits the waves into the soil, which is generally regarded as an infinite space, and these waves are not returning back. The vibration energy is therefore dissipated, and damping is introduced into structure-soil system. This damping is called radiation damping. In addition to this, soil has its own material damping, changing the response of the system even further. To summarize in few words - dynamic soil-structure interaction is the conjunction of structure and soil when subjected to dynamic excitation, where dynamic properties of both, the structure and the soil, are significantly changed due to the dynamic interaction between them.
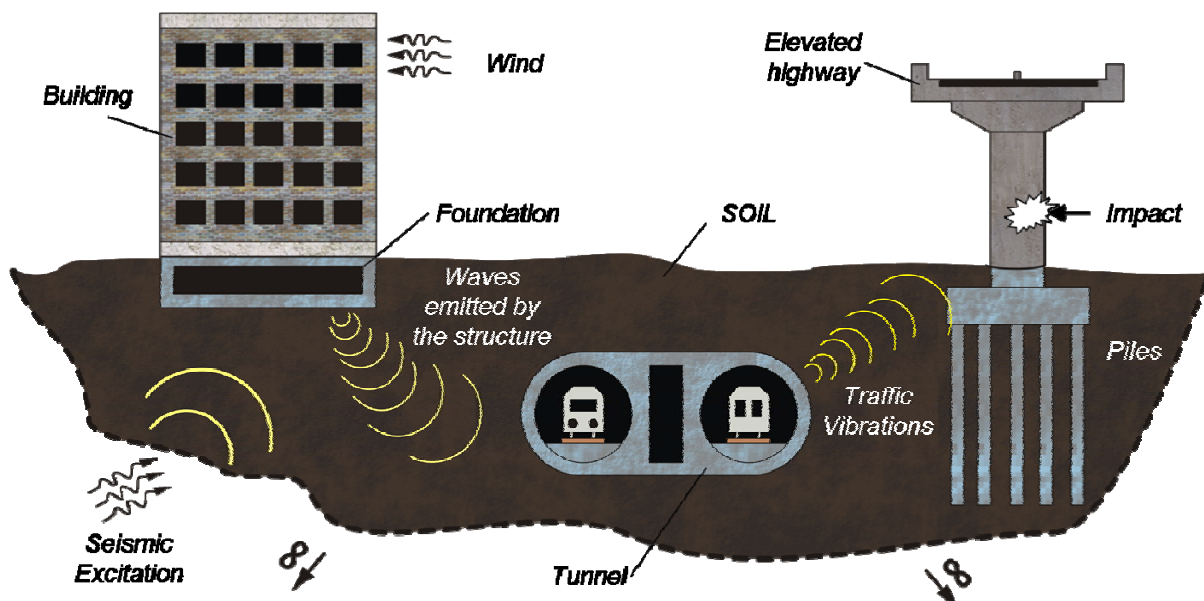

Figure 1: *Typical examples of dynamic soil-structure interaction*

Other typical soil-structure interaction examples, like traffic induced vibrations or oscillations of structures founded on the soft soil and subjected to wind or impact loading, can be seen in the *Figure 1*. Dynamic loads can act directly on the structure (wind, rotating machinery, impact loads) or they can be introduced into the system trough soil (earthquake, underground traffic).

When people think about dynamic SSI, they usually think of the favorable influence that it has on the dynamic behavior of the structure (higher damping). This brings them to the *wrong* conclusion that this phenomenon can be neglected ("safe side approach"). As the contra example we have the case of a collapse of the famous Hanshin Expressway during the Kobe earthquake. Previously many have argued that the collapse and the destruction of *18* piers were results of the poor deign of the structure, mainly the lack of lateral confinement in the piers. In their study, *Mylonakis et al.* [8] have shown that the structure would have collapsed even if the modern regulations for the design had been used. They showed that the main reason for the collapse was the neglection of the SSI effect. Due to SSI, the fundamental period was elongated for *20%*, bringing the structure into the dangerous zone of strong ground motions. This resulted in *50%* increase in ductility demand for the piers, in contrast to the solution where the piers are assumed to be fixed to the ground.

The analysis of the dynamic behavior of the structure does not follow the logic of safety factors used in static analysis. The true nature of the behavior of structures under dynamic excitation is a complex matter and the results can often be non-intuitive and very hard to predict, even for an experienced structural analyst.

2. STATEMENT OF THE PROBLEM

There are two general approaches to model soil-structure interaction - direct and substructure method. In the first, direct approach finite part of the unbounded soil is modeled together with the structure, most commonly with finite elements (*Figure 2(a)*). The waves propagate from the structure into the finite soil medium, and a significant portion of the energy is taken away from the structure. In the direct method, the waves are reflected from the artificially induced boundaries, causing the energy to return to the structure. To prevent this, some form of boundary condition is established trying to absorb or to transmit the waves. To decrease the influence of these boundaries, a large portion of the soil usually has to be modeled. Thus the number of degrees of freedom of the soil will significantly surpass the number of the degrees of freedom of the structure, especially for three-dimensional problems.
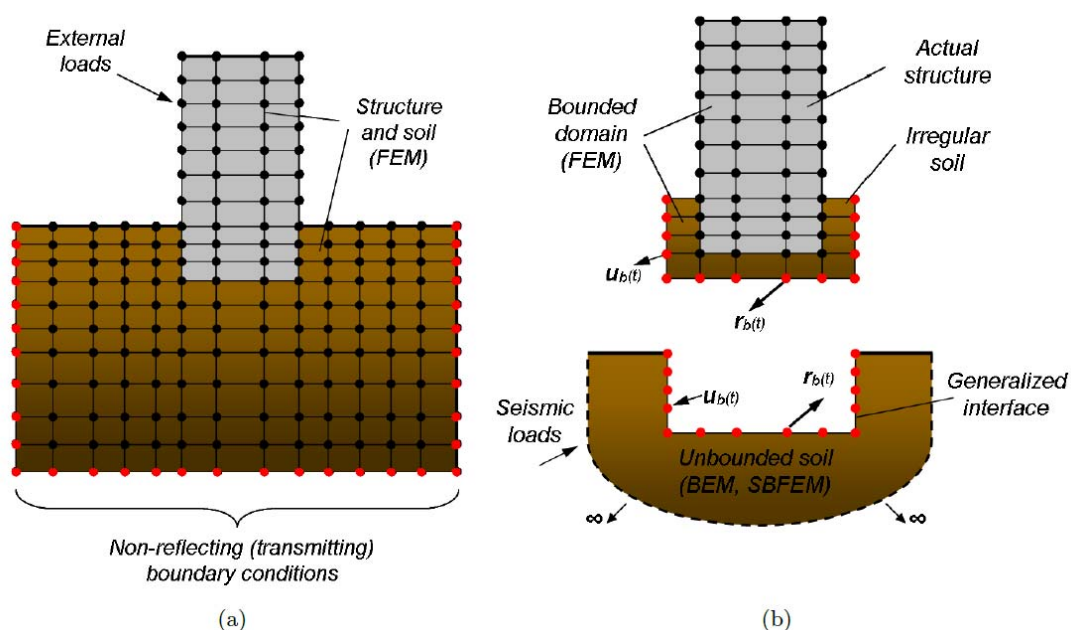

Figure 2: *(a) Direct method (b) Substructure method*

In the second approach bounded and unbounded parts are modeled as two substructures separated by the generalized soil-structure interface. Bounded substructure consists of the actual structure and a portion of the soil with irregular boundaries, which can exhibit non-linear behavior (in further referenced as structure). The unbounded substructure consists of the remaining part of the soil stretching to infinity and assumed to be linear (in further referenced as soil). Unbounded soil is generally assumed as linear (*Figure 2(b)*).

The connection between the two substructures is assured by the ground interaction forces $\mathbf{r_b}(t)$ acting in opposite directions on the soil and on the structure (*Figure 2(b)*). The interacting force-acceleration relationship for the soil in time domain can be represented by the convolution integral

$$\mathbf{r_b}(t) = \int_0^t \mathbf{M_b^\infty}(t)\ddot{\mathbf{u}}(t-\tau)d\tau ,$$

where $\mathbf{M_b}^\infty(t)$ denotes the acceleration unit-impulse response matrix. The subscript *b* denotes the nodes that lay in the soil-structure interface, which belong to both, the structure and the soil.

To solve the soil-structure interaction problem by the substructure approach in time domain, the acceleration unit-impulse response matrix $\mathbf{M_b}^\infty(t)$ must be determined.

3. SCALED BOUNDARY FINITE ELEMENT METHOD

Scaled boundary finite element method (SBFEM) is a substructure method, first developed by *Wolf and Song* [12]. This method combines good characteristic of both the finite element and the boundary element method [13]. No fundamental solution is needed, but the radiation condition is satisfied exactly. Only the boundary is discretized using standard line or surface finite elements, leading to the reduction of the dimension of the problem by one. Coupling with the finite-element method is straightforward. The governing equations of motion are exact in radial direction, while the finite element approximation is applied in the circumferential directions.

SBFEM is global in space and time which means that the response of a certain point in space depends on the response of all the other points (spatially global) for the entire time history prior to the observed time (temporally global). This implies that the acceleration unit-impulse response matrix $\mathbf{M_b}^\infty(t)$ is fully populated and the convolution integral has to be evaluated over the entire time for every single time step to determine it.

Soil can be modeled as non-homogeneous, with modulus of elasticity and mass density varying as power function of spatial coordinates [1][2][3]. Thus the natural sedimentation process of soil can be modeled without additional effort (*Figure 3*).
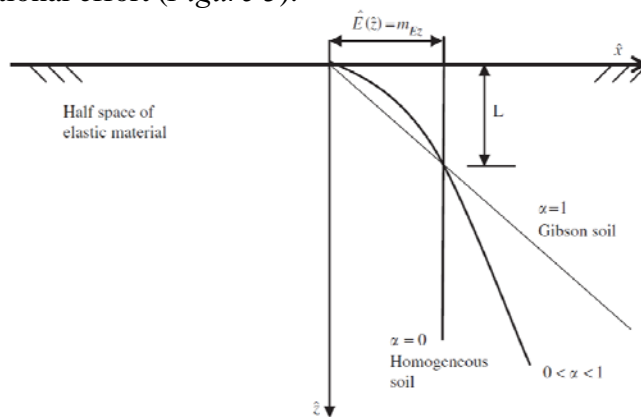

Figure 3: *Variation of modulus of elasticity as power function of depth [1][2][3]*

Two essential improvements have been developed and implemented to improve the performance of the general SBFE method in time domain.

First issue is the computation of $\mathbf{M_b}^\infty(t)$. The original discretization scheme [2][3][12][13] assumes a constant change of the $\mathbf{M_b}^\infty(t)$ within each time step and is only conditionally stable. A rather small minimum step size leads to a computationally very demanding procedure. A new discretization scheme for the solution of the SBFEM equations assumes the acceleration unit-impulse response matrix to vary linearly within each time step and an extrapolation parameter is introduced to provide stability. For large problems the linearization of the acceleration unit-impulse response matrix for late times, similar to what has been proposed by *Zhang et al.* [15], *Lehmann* [4][5] and *Yan et al.* [14], is employed. Together with the new discretization scheme, this presents a very fast, accurate and robust approach.

The second issue concerns the calculation of the soil-structure interaction load vector $\mathbf{r_b}(t)$. Based on integration by parts, a new and very efficient integration scheme for the evaluation of the convolution integral is developed, regaining a strong locality in time and providing a reliable control of the cut-off-errors. [16]

The combination of these enhancements leads to a very significant reduction of computational effort and linear dependency with respect to the number of time steps, and allows also the use of larger time steps. Examples analyzed by authors did not show instability of the solution for a wide range of parameters. The method thus has become mature for a wide range of problems.

4. EXAMPLE 1

In this 2D example the comparison between the classical direct approach for modeling the soil-structure interaction using *viscous boundary* [6][7][10][11] and SBFE method will be presented.

Foundation is a strip foundation analyzed on the assumption of the plane strain condition. Cross section area is *2B x H = 5.0 x 1.0 m*. The elastic properties of the foundation are given in the *Figure 4*, and of the soil in the *Figure 5*. The soil is homogeneous. The foundation is set to be massless. Foundation is discretized with quadrilateral finite-elements of the size *0.25 x 0.25 m*. For the SBFEM solution (*Figure 4*), line SB finite-elements are applied on the boundary where the foundation is in contact with the soil. Scaling point *O* coincides with the origin of the coordinate system. For the direct method solution, the viscous boundary is applied at the distance of *5xB*, *10xB* and *20xB* from the origin of the coordinate system (*Figure 5*). The damper constants are determined from the following expressions

$$c_n = A \cdot \rho \cdot c_p; \quad c_t = A \cdot \rho \cdot c_s,$$

where c_n and c_t represent the damping constants in normal and transversal direction to the boundary, and c_p and c_s the dilatational and shear wave velocity of the soil.

Triangular impulse load is applied in point *A* ($P_0 = 10^5 kN$). The vertical displacement of the point *B* is recorded for the time history *4000 x Δt*, where *Δt = 2.5 x 10^{-3} s*. For the SBFEM solution, *100* acceleration unit-impulse response matrices $\mathbf{M_b}^\infty(t)$ with the time step size *5 x Δt* are computed, before the linearization is applied.
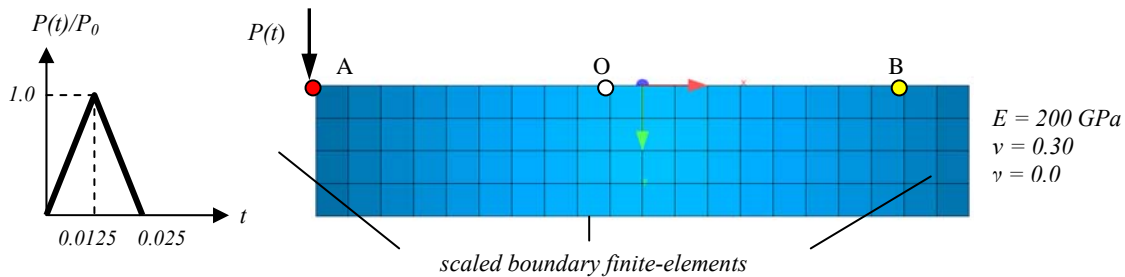

Figure 4: *Substructure method with scaled boundary finite-elements at the soil-foundation interface*
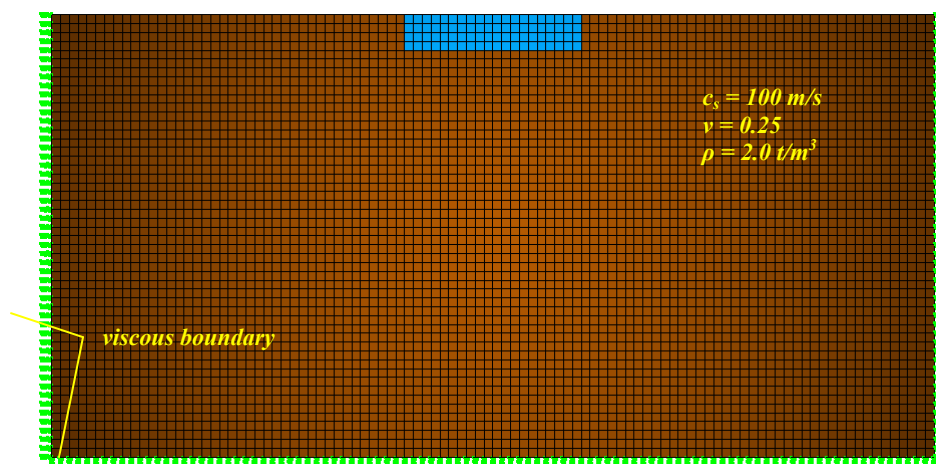

Figure 5: *Direct method with viscous boundaries (5 x B)*

As can be seen from the *Figure 6a-b*, the solution with the viscous boundaries depends on the distance between these boundaries and soil-structure interface. The viscous boundaries are the exact solution to the body wave propagation problem when the wave is arriving on the boundary under

the 90^0 angle (1D solution). In real 2D or 3D problems this never occurs, there will always be some reflection from the boundary, as well as the presence of surface waves. For a more distant boundary the angle of incidence will be closer to 90^0 degrees, and more energy will be absorbed. This can be seen on the *Figure 6b*, where approximately at the times *0.2s*, *0.4s* and *0.8s* (for the solution *5xB*, *10xB* and *20xB* boundary distance respectively), we have body wave reflected from the boundary arriving on the observation point *B*. After a while, the reflected waves will lose their energy and will be absorbed by the viscous boundary. In addition to this, solution with the viscous boundaries will always produce some constant displacement (*Figure 6a*) [11].
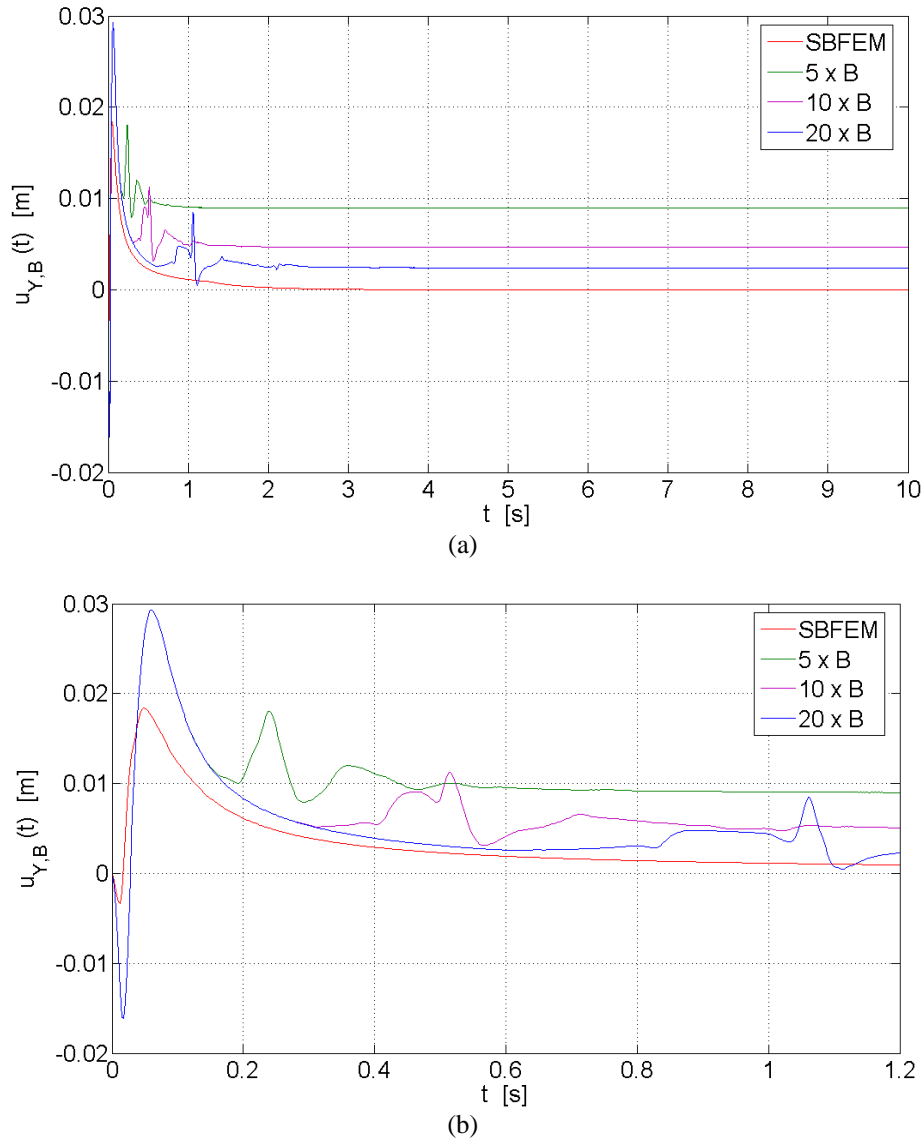

(a)

(b)

Figure 6: *(a) Displacement time history of the point B (b) Early time (zoom)*

The SBFEM solution is an accurate solution in finite-element sense of the word - it approaches the exact solution by increasing the number of the elements on the boundary. As can be seen from the *Figure 6a-b*, no reflection of waves occurs. Total computational time for the SBFEM solution is *18s*, compared to the *129s*, *625s* and *3807s* which takes the solution with viscous boundaries to be computed (for the model size *5xB*, *10xB* and *20xB* respectively).

Radiation damping that the soil is introducing into the system here is quite large. Only a few oscillations are present. At the beginning, point *B* moves upwards. This is the consequence of the eccentrically applied load, and upward movement of the point *B* is the result of the rotation of the foundation (no-tension condition for the uplift of the foundation is not accounted for). After a certain time, the entire foundation starts to move downwards.

5. EXAMPLE 2

This 2D plane strain example of road-tunnel traffic system is intended to show the propagation of waves in more complex environment. The reference example can be found in *Lehmann* [5].

The geometry and material properties of the model are shown in the *Figure 7*. Near field (structure) is modeled with 4-node quadrilateral finite-elements, while the far field (unbounded soil) is modeled with 2-node line scaled boundary finite-elements. SB finite-elements are applied at the interface between near and far field.

System has been analyzed under the step load show in the *Figure 7*. The vertical displacement of the observation point is recorded for the total time history $6000 \ x \ \Delta t$, where $\Delta t = 2.5 \ x \ 10^{-4} \ s$. Before the linearization is applied, 40 acceleration unit-impulse response matrices $\mathbf{M_b}^{\infty}(t)$ with the time step size $40 \ x \ \Delta t$ are computed.

- tunnel: $E= 30 \ GPa, \ v=0.33, \ \rho=2.0 \ t/m^3$
- building: $E= 3 \ GPa, \ v=0.30, \ \rho=2.0 \ t/m^3$
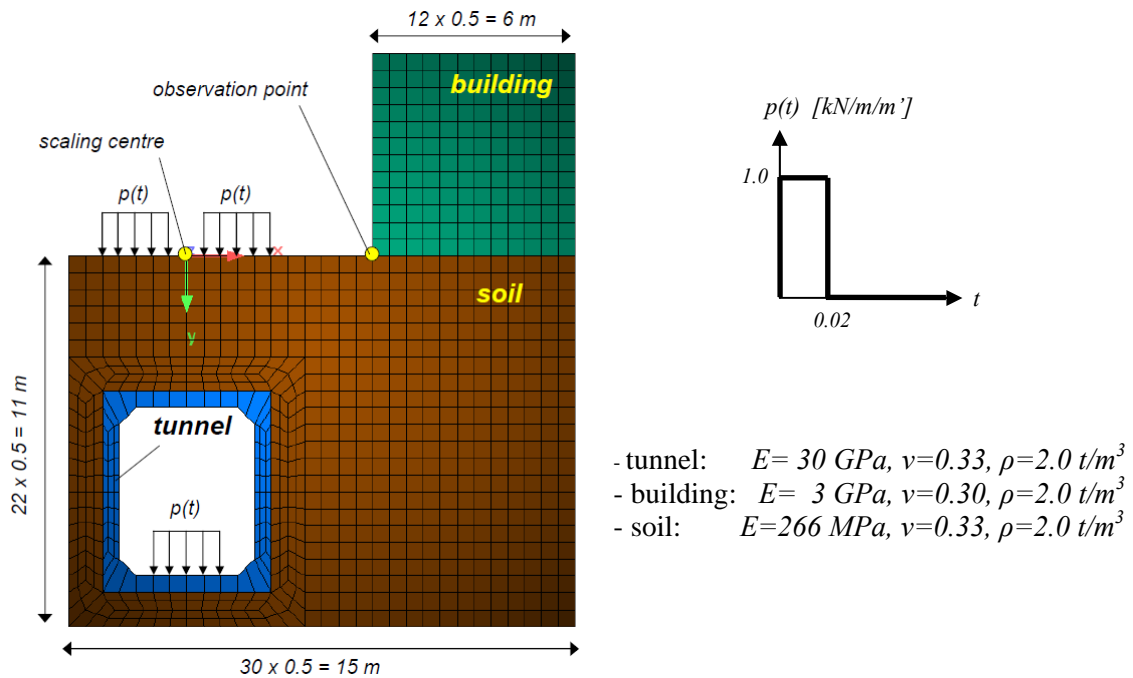- soil: $E=266 \ MPa, \ v=0.33, \ \rho=2.0 \ t/m^3$

Figure 7: *Road-tunnel traffic system*

The results are displayed in the *Figure 8a-b*. It takes some time for a wave to reach the observation point (*Figure 8b*). Shear (S) and dilatational (P) wave velocities of the soil are $c_s=224 \ m/s$ and $c_p=386$ m/s, while the shortest distance from the excitation point to the observation point is *3m*. The time that it takes for S and P wave to reach the observation point is *0.013s* and *0.008s*, respectively. After some *4-5* periods of vibration, no more oscillations exist (*Figure 8b*).
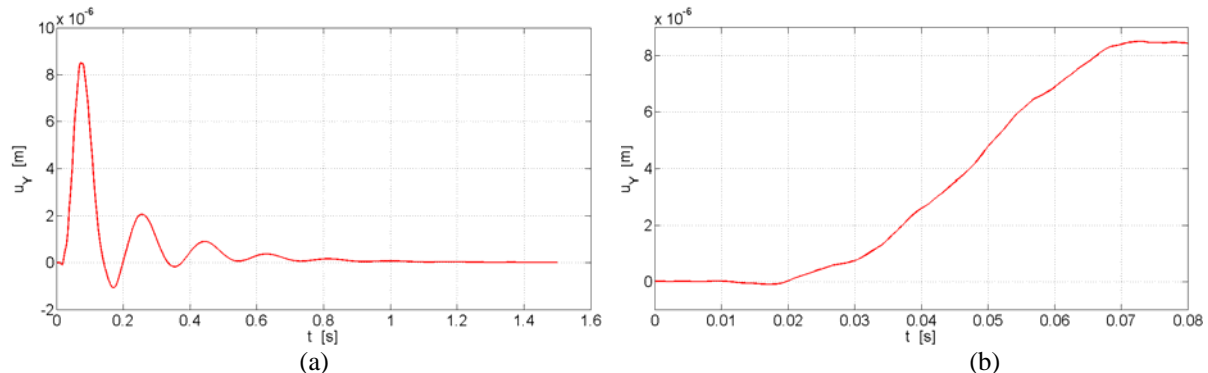
(a)

(b)

Figure 8: *(a) Vertical displacement history (b) Early time (zoom)*

6. EXAMPLE 3

The following example [9] shows a more moderate, but still important influence of the soil on the dynamic behavior of the structural system. A water tower subjected to the horizontal blast load is analyzed.

Geometry of the system is displayed in the *Figure 9a*. Foundation is mass less and has stiffness which is much larger than the stiffness of tower and the soil. Soil is modeled with 4-node quadrilateral SB finite elements, which are applied on the foundation-soil interface (*Figure 9b*).

The response of the soil-structure system is calculated for the time-history in the duration of *1.0* second. Total number of time steps is *400*, while the time step size *Δt* equals *0.0025s*. Horizontal blast load in the direction of *x-axis* is applied to the system at the top of the tower. Load is modeled as a symmetric triangular impulse in the duration *0.05s*.
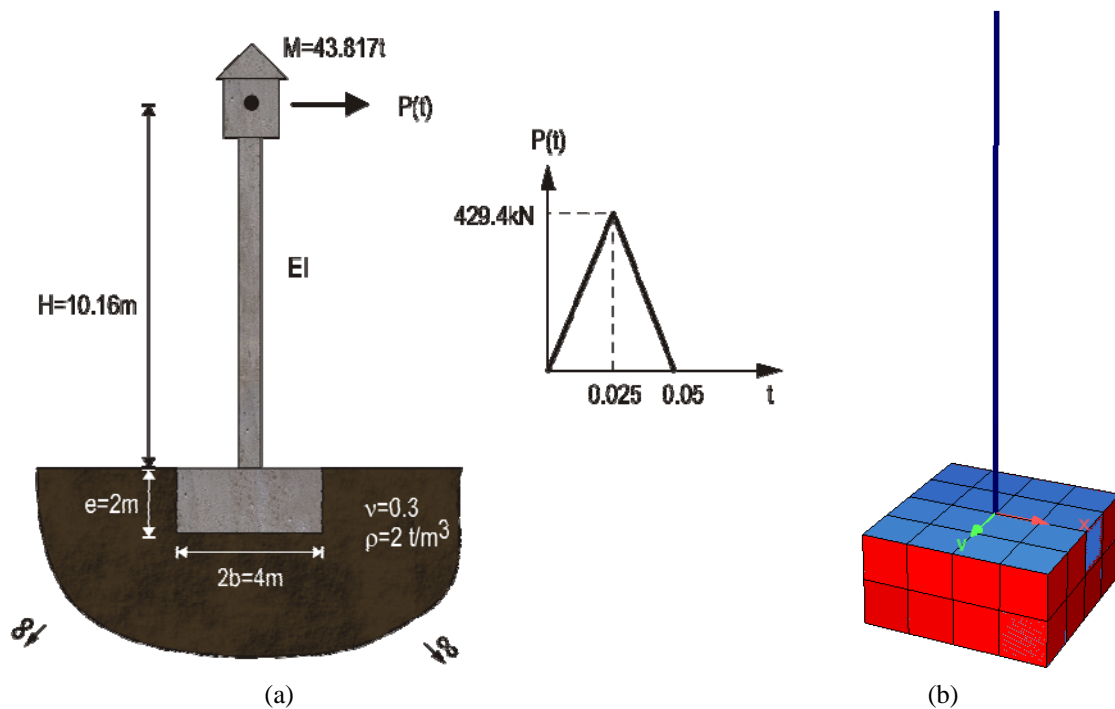

Figure 9: *(a) Water tower-soil system (b) 3D FE and SBFE model of the soil-structure system. Blue elements represent the structure part while red SBFE quadrilaterals represent the soil.*

Figure 10-Figure **11** show time history of the horizontal displacement response of the top of the water-tower, in the direction of the load applied. *Figure 10* illustrates the influence that the stiffness of the soil has on the response of the soil-structure system. The results for three different cases are displayed. First corresponds to the case when the soil is much stiffer than the structure, which means that it can be assumed that the structure is rigidly founded in the soil. The response completely depends on the dynamic characteristics of the structure. No damping is present. In the second case ($c_s = 200m/s$), the characteristics of the soil are such that the contribution of the soil to the dynamic response of the soil-structure system cannot be neglected. The period of oscillation is longer and the damping appears. Since no material damping of the soil and the structure is modeled, damping is completely the result of the waves propagating into infinite soil medium and not returning back (radiation damping). Third case corresponds to even softer soil ($c_s = 100m/s$) where the influence of the soil on the dynamic characteristics of the soil-structure system are apparent.
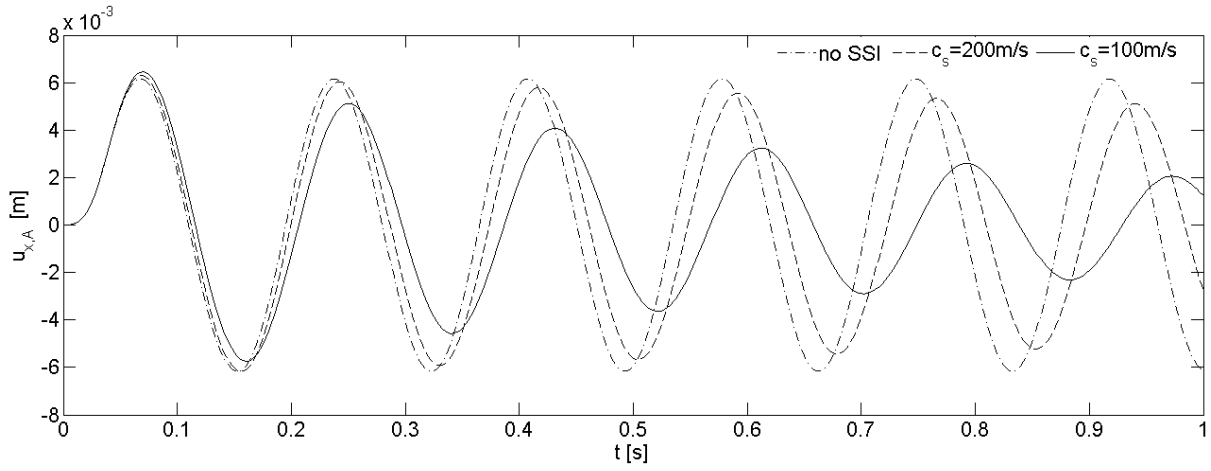
Figure 10: *Time history of the horizontal displacement response at the top of the tower: Influence of the soil flexibility on the dynamic characteristics of the soil-structure system.*

Figure 11 illustrates the damping properties of this soil-structure system in more detail. The envelopes of the amplitudes (dotted lines) are determined assuming that the soil-structure system is behaving as the single degree of freedom system with viscous damping, oscillating in steady-state. Assuming that the damping is small, the decay constant $\varepsilon = c/2m$ and percentage of critical damping $\xi = c/c_{crit}$ can be determined as follows

$$\xi = \frac{1}{2\pi s} \ln\left(\frac{y_0}{y_s}\right); \quad \varepsilon = \frac{1}{sT_d} \ln\left(\frac{y_0}{y_s}\right),$$

with y_0 and y_s denoting the amplitudes of the vibration at time stations t_0 and $t_s = t_0 + sT_d$, T_d damped period of oscillations and s number of periods between two time stations. The envelopes are then described by the function $\pm C \cdot e^{-\varepsilon t}$. The values of C and ε are displayed in the *Figure 11*. The envelopes plotted below indicate good agreement between the assumed damping model and the "real" damping of the soil-structure system.
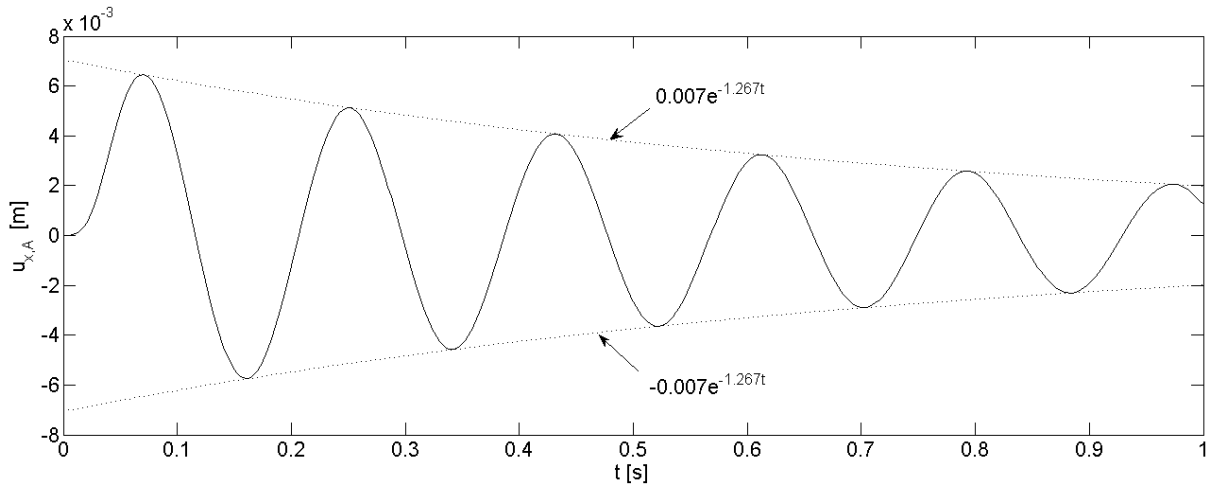

Figure 11: *Time history of the horizontal displacement response at the top of the tower: Amortization of the oscillations of the soil-structure system as a result of the radiation damping.*

The influence of the stiffness of the structure and soil flexibility on the fundamental circular frequency of the soil-structure system ω_s and the radiation damping ξ *is* plotted in the following figures. *Figure 12* shows the radiation damping ξ versus the fundamental period of the structure T_e founded on the rigid rock. We can see that the soil can introduce significant damping into the soil-structure system. Damping depends on the soil characteristics as well as the stiffness of the structure. Even for relatively soft soil ($c_s = 100m/s$), radiation damping will become neglectable for the structures with moderate flexibility. But for stiff structures on a soft soil it will be of importance.
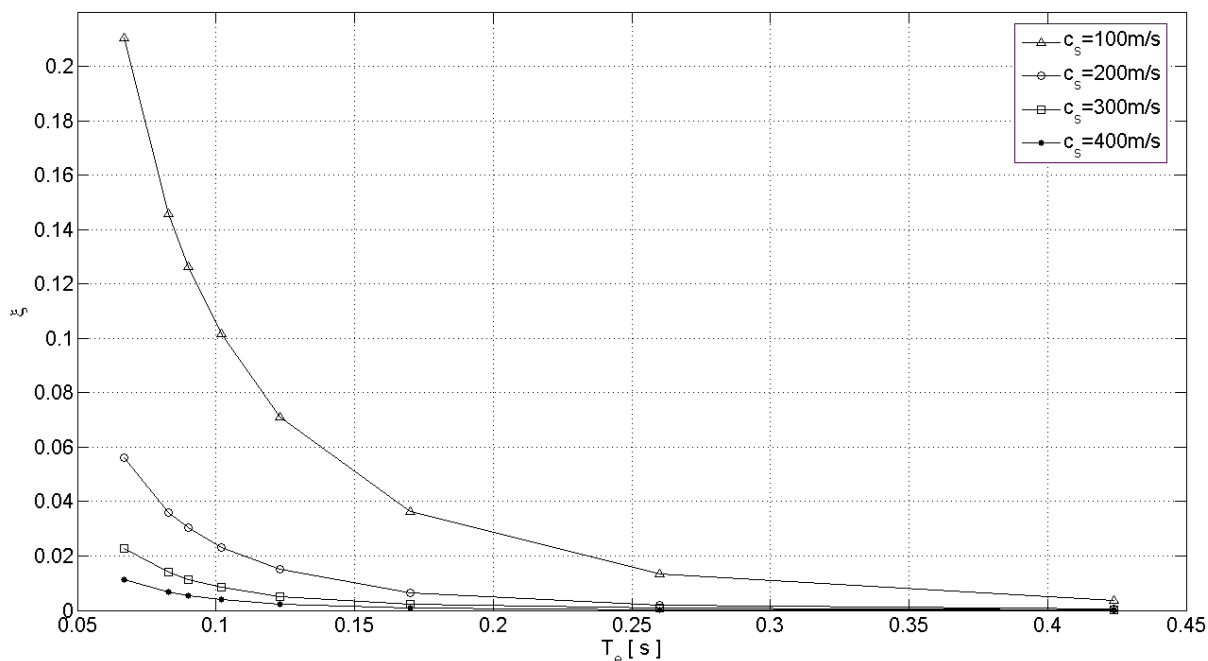
Figure 12: *Influence of the stiffness of the structure and soil flexibility on the radiation damping*

Figure 13 illustrates the influence of the soil-flexibility and stiffness of the structure on the fundamental frequency of the soil-structure system. It can be concluded that the higher the ration between the stiffness of the structure and the stiffness of the soil, the smaller is the fundamental frequency of the soil-structure system. For moderate to high stiff structures soil-structure interaction plays no role on their dynamic behavior.
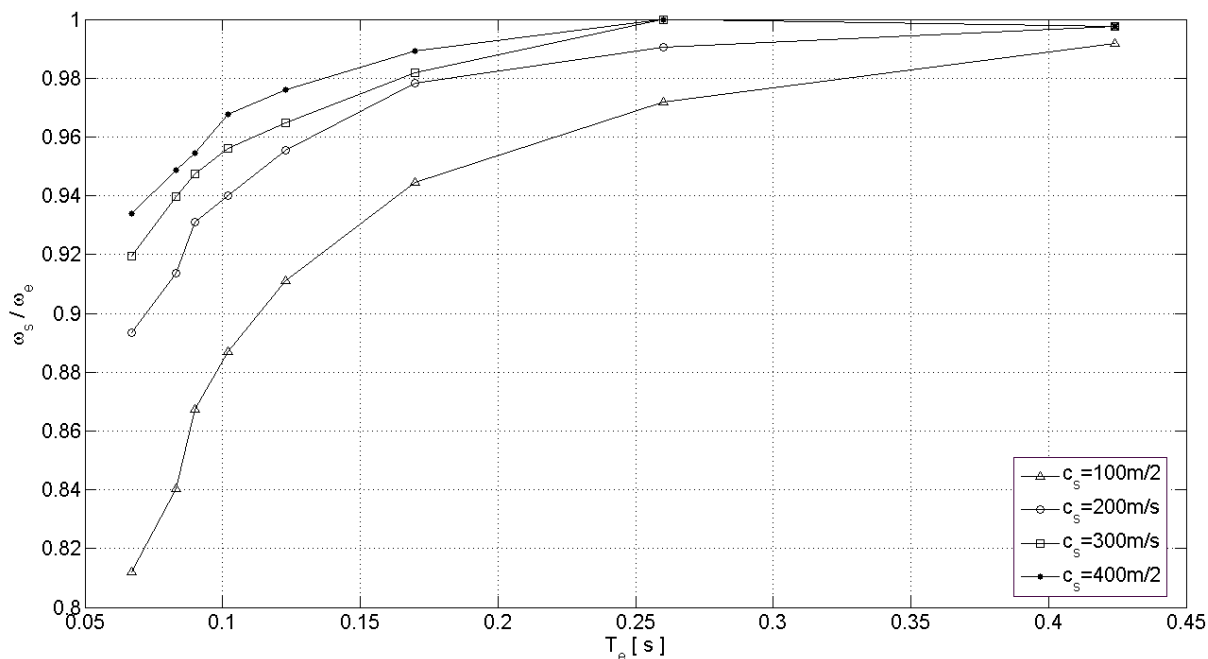

Figure 13: *Influence of the stiffness of the structure and soil flexibility on the fundamental frequency of the soil-structure system*

Simplified solutions based on a circular foundation have been developed by Lysmer, Yamahara and others, which can be used for an estimate of the response for lower frequencies [17]. Based on the mass ratio we get stiffness and damping constants for a simple one point spring/damper element. The results are similar for that case, but they show larger displacements because this solution assumes a foundation on top of the soil, while the SBFEM solution is embedded in the soil.
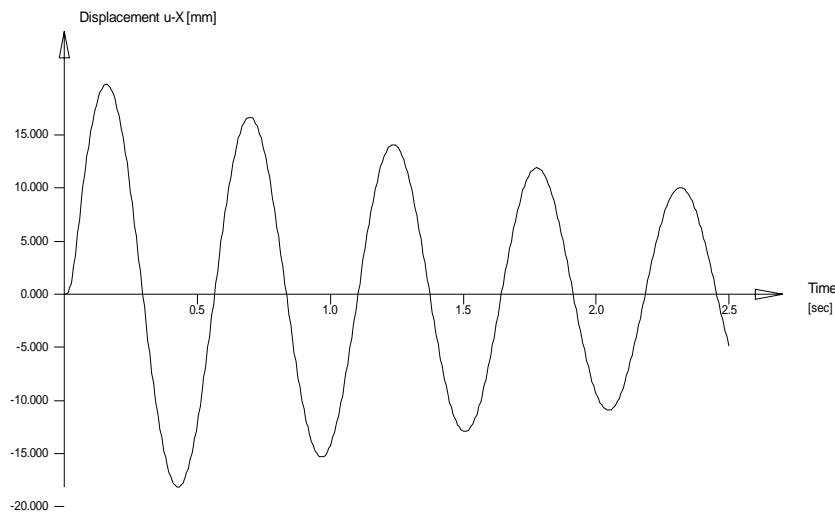
Figure 14: *Results of simplified analysis with single spring elements*

The implementation of the SBFEM within SOFiSTiK module DYNA (12.70) has achieved some very important modifications increasing the efficiency of the method by magnitudes. Thus the handling of dynamic soil structure interaction has become now possible to a greater extent.

The handling of the method is quite simple. The user selects a group of edges in 2D or surface elements in 3D as the interface to the soil structure (GRP *nn* SOIL). The soil is assumed to be on the right of the edge resp. in the local +z direction of the QUAD. The scaling point is assumed in the top most location with the mean value of the horizontal coordinates, but may be overwritten by discrete node number NSCP. Special variations of the material parameters may be defined with SMAT records.
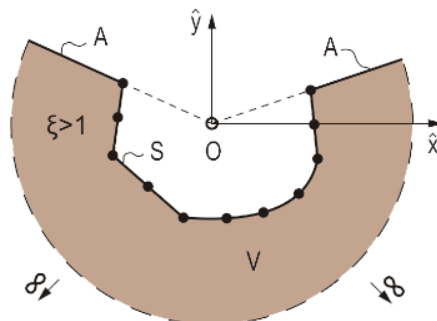

Figure 15: *Scaling point and boundary conditions*

We have then the number of time steps in the STEP record of the analysis itself. The user may define then an integer factor DTF on the step size to be used for the unit impulse matrix, and the number M of matrices to be used by a frequency EIGS = 1/(M*DTF*Δt).

Compared to single spring elements the method provides higher precision, compared to direct methods it is faster and avoids any reflection at the far boundaries. But there are some limits to keep in mind. As the radial expansion relies on a scaling point, the description of layered soils is not possible. So the general usage will describe the local effects with a small direct finite element region and apply the SBFEM for the boundary condition of that region.

7. REFERENCES

[1] *J.R. Booker, N.P. Balam, and E.H. Davis*. The behavior of an elastic nonhomogeneous half-space. International Journal for Numerical and Analytical Methods in Geomechanics, 9:353-381, 1985.

[2] *M.H. Bazyar and C. Song.* Time-harmonic response of non-homogeneous elastic unbounded domains using the scaled boundary finite-element method. Earthquake Engineering and Structural Dynamics, 35:357-383, 2006.

[3] *M.H. Bazyar and C. Song*. Transient analysis of wave propagation in non-homogeneous elastic unbounded domains by using the scaled boundary-finite element method. Earthquake Engineering and Structural Dynamics, 35:1787-1806, 2006.

[4] *L. Lehmann*. An effective finite element approach for soil-structure analysis in the time domain. Structural Engineering and Mechanics, Vol 21, No 4, 2005.

[5] *L. Lehmann*. Wave Propagation in Infinite Domains: With Applications to Structure Interaction. Springer-Verlag, Berlin, Heidelberg, 2007.

[6] *J. Lysmer and R.L. Kuhlemayer*. Finite dynamic model for infinite media. Journal of the Engineering Mechanics Division, 95:859-877, 1969.

[7] *J. Lysmer and G. Waas*. Shear waves in plane infinite structures. Journal of the Engineering Mechanics Division, 98:85-105, 1972.

[8] *G. Mylonakis, C. Syngros, G. Gazetas and T. Tazo*. The role of soil in the collapse of 18 piers of Hanshin Expressway in the Kobe earthquake. Earthquake Engineering and Structural Dynamics, 35:547-575, 2006.

[9] *B. Radmanovic*. Evaluation of Dynamic Soil-Structure Interaction in Frequency and Time Domain. MSc Thesis. Technical University of Munich. 2009.

[10] *J.P.Wolf*. Dynamic Soil-Structure-Interaction Analysis. Prentice-Hall, Englewood Cliffs, NJ., 1985.

[11] *J.P.Wolf*. Soil-Structure-Interaction Analysis in Time Domain. Prentice-Hall, Englewood Cliffs, NJ, 1988.

[12] *J.P. Wolf and C. Song*. Finite-Element Modelling of Unbounded Media. John Wiley and Sons, Chichester, England, 1996.

[13] *J.P. Wolf*. The Scaled Boundary Finite Element Method. John Wiley and Sons, Chichester, England, 2003.

[14] *J. Yan, C. Zhang, and F. Jin*. A coupling procedure of FE and SBFE for soil-structure interaction in the time domain. International Journal for Numerical Methods in Engineering, 59:1453-1471, 2004.

[15] *X. Zhang, J.L. Wegner, and J.B. Haddow*. Three-dimensional dynamic soil-structure interaction analysis in the time domain. Earthquake Engineering and Structural Dynamics, 28:1501-1524, 1999.

[16] *B. Radmanovic, C. Katz*. High Performance SBFEM, WCCM Sydney, 2010

[17] *J.A. Studer, J.Laue, M.G.Koller*, Bodendynamik, Springer, Berlin, 2007